Original Article

Mechanical and fatigue properties of long carbon fiber reinforced plastics at low temperature

Mitsuhiro Okayasu[*], Yuki Tsuchiya

Graduate School of Natural Science and Technology, Okayama University, 3-1-1 Tsushimanaka, Kita-ku, Okayama, 700-8530, Japan

ABSTRACT

The mechanical properties of long unidirectional (UD) and crossply (CR) carbon fiber reinforced plastics (CFRPs) were investigated at a low temperature (-196 °C). The CFRPs were fabricated from 60 vol.% carbon fiber and epoxy resin. The bending strength of the UD-CFRP was approximately twice that of the CR-CFRP. The high strength of the UD-CFRP was directly attributed to the amount of carbon fiber oriented along the loading direction: 60% for UD-CFRP compared with 30% for CR-CFRP. The low-temperature (-196 °C) tensile and fatigue strengths of the UD-CFRP were over 1.5 times greater than those at room temperature (20 °C). This was attributed to the increased epoxy strength at low temperatures along with the internal compressive stress arising from the different thermal expansion coefficients of the carbon fiber and epoxy. Both the epoxy strength and internal compressive strength were employed as factors in a compound law to numerically estimate the low-temperature tensile strength. This work presents a systematic analysis for changes in the CFRP material properties at low temperatures.
© 2019 Publishing services by Elsevier B.V. on behalf of Vietnam National University, Hanoi. This is an open access article under the CC BY license (http://creativecommons.org/licenses/by/4.0/).

1. Introduction

The utilization of composite materials, especially carbon fiber reinforced plastics (CFRPs), has dramatically increased in recent years because of their low specific weight and high specific strength. In particular, CFRP materials have received considerable attention because of their practical use in the aerospace industry. Spacecraft fly in the atmosphere and the surrounding space (e.g., 100 km above the ground), where the air pressure is too low to maintain lift and the air temperature changes dramatically within the range of -100 to 100 °C. To ensure spacecraft safety, it is necessary to examine the material properties of CFRPs at low and high temperatures.

The material properties of CFRPs and related information have been reported in past studies. Puente et al. [1] examined damage in quasi-isotropic and woven carbon fiber/epoxy laminates caused by intermediate- and high-velocity impacts at low temperatures. Dutta et al. [2] analyzed the energy absorption of graphite/epoxy plates under low-velocity impacts using a Split—Hopkinson pressure bar and found a small dependence on temperature in the range of -69 to 20 °C. Although the mechanical properties of CFRPs at low temperatures have been reported, no study has analyzed the factors underlying the effects of temperature on their mechanical properties.

Understanding the fatigue properties of engineering materials is important in the design process since over 90% of component failures are caused by fatigue. Several studies have focused on the deterioration of CRFPs through fatigue. The fatigue life of a unidirectional CFRP was predicted at temperatures greater than 100 °C, and the results showed a significant decrease in the fatigue strength at high temperatures [3]. The fatigue strength of CFRPs can be directly attributed to defects (e.g., voids and cracks) caused by high stress concentrations [4]. The fatigue strength of CFRPs with short carbon fibers [5] was reported to increase with a greater carbon fiber content, which is correlated with its tensile strength. The fatigue strength of CFRPs with short carbon fibers was also affected by the extent of residual stress arising from crack closures. To obtain high fatigue strength, Huawen et al. [6] prepared CFRP laminates in which pre-stressed CFRP plates were attached to mild steels. They found that increasing the pre-stressing level increased the fatigue life of the CFRP plate.

The fatigue properties for CFRPs have been investigated using various experimental approaches, which have provided useful information when designing engineering components. However, the lack of related studies in the literature suggests it is still necessary

---

* Corresponding author. Fax: +81 86 251 8025.
E-mail address: mitsuhiro.okayasu@utoronto.ca (M. Okayasu).
Peer review under responsibility of Vietnam National University, Hanoi.

to examine the fatigue properties of CFRPs at low temperatures in relation to service conditions for applications in the aerospace industry [7]. In particular, further information on the failure characteristics of CFRPs at low temperatures is needed. Therefore, this study investigates the tensile and fatigue properties both experimentally and numerically at low temperatures. Furthermore, a new compound law is proposed to accurately estimate the associated mechanical properties.

2. Experimental

2.1. Materials and experimental conditions

The mechanical properties of commercial unidirectional (UD) and crossply (CR) CFRPs (UD-CFRP and CR-CFRP, respectively) with a thermoset resin (epoxy) were investigated. The carbon fiber used in this study was T303 (TORAY Industries, Inc.). Fig. 1 shows photographs of the sheet-shaped UD-CFRP and CR-CFRP specimens, indicating different textures for the carbon fiber between the specimens. The carbon fiber content of the CFRPs was 60 vol.%, and the CFRP sheets were produced with thicknesses of 1 mm using a hot-pressing process. The bending, tensile, and fatigue strengths of the CFRPs were evaluated at both room temperature (20 °C; T_1) and low temperature (-196 °C; T_2). The CFRP samples were immersed directly in liquid nitrogen using a special container to cool them down to -196 °C.

Fig. 2 shows schematic diagrams of the experimental setups used to evaluate the mechanical properties of the CFRP samples: three-point bending test, tensile test, and fatigue test in liquid nitrogen. Containers made of stainless steel and Styrofoam were employed because of their desired resistances to high and low temperatures. The bending and tensile tests were conducted using a screw-driven universal testing machine with a capacity of 50 kN. The specimens were loaded with a stroke control at a rate of 1 mm/min until fracture. The applied load and strain were measured using a load cell and strain gauge, respectively. The fatigue tests were performed using an electro-hydraulic servo system with a capacity of 50 kN. During fatigue testing, the relationship between the stress amplitude (S_a) and the cycle number to final fracture (N_f) was evaluated. Tensile–tensile loading at a load ratio of 0.1 and a frequency of 30 Hz was applied to the test specimens until they completely fractured or their endurance limit was reached at 10^5 cycles.

2.2. Strain analysis

To clearly reveal the CRFP material properties at low temperatures, strain measurements were carried out using commercial
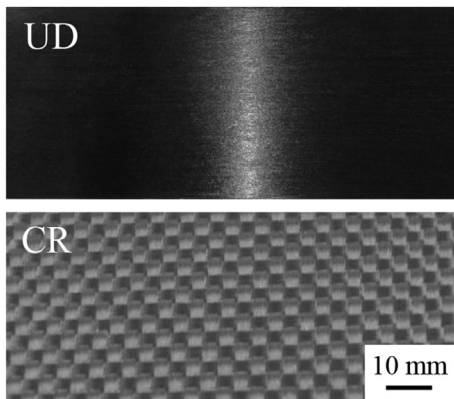

Fig. 1. Photographs of the UD-CFRP and CR-CFRP composites containing a thermoset resin (epoxy).

strain gauges with 2-mm lengths. Fig. 3 shows a schematic illustration of the CFRP sample with attached strain gauges. Three commercial strain gauges were attached to the surface and inside of the CFRP specimens with different orientations (e.g., parallel and perpendicular to the carbon fiber direction). It is noted that the surface and interior of the CFRP specimens were dominated primarily by epoxy and carbon fibers, respectively.

Numerical analyses (three-dimensional finite element (FE) simulations with eight-node quad elements) using commercial software (ANSYS 15.0) were conducted to examine the internal strain at -196 °C. The mesh sizes of the carbon fibers and the surrounding epoxy were determined to be less than 0.01 mm. The material parameters for the numerical analysis were: elastic constant $E_f = 230$ GPa, Poisson ratio $\nu_f = 0.30$, and thermal expansion coefficient $\alpha_f = -0.4 \times 10^{-6}/°C$ for the carbon fiber; and $E_m = 2.4$ GPa, $\nu_m = 0.3$, and $\alpha_m = 50 \times 10^{-6}/°C$ for the epoxy [8].

3. Results and discussion

3.1. Mechanical properties

Fig. 4 shows the bending strengths for the CR-CFRP and UD-CFRP at 20 °C (T_1) and -196 °C (T_2). The bending stress was calculated as:

$$\sigma_{bend} = M_{max}/Z \tag{1}$$

$$= 3Pl / 2bh^2 \tag{1a}$$

where M_{max} is the maximum bending moment, Z is the section modulus, P is the applied load, l is the span for the bending load, and b and h are the width and height of the CFRP specimen, respectively. As shown in Fig. 4, the bending strength for the UD-CFRP was approximately two times that of the CR-CFRP. This result may be related to the amount of carbon fiber in the loading direction (60% for UD-CFRP vs. 30% for CR-CFRP). In addition, the bending strengths for both types of CFRPs were approximately 1.5 times higher at -196 °C than at room temperature. Tensile tests were conducted to further verify the high strength of the CFRPs at low temperatures.

Fig. 5(a) shows the relationships between the engineering tensile stress and strain for the UD-CFRP at 20 and -196 °C, and the ultimate tensile strengths are summarized in Fig. 5(b). The tensile strength (σ_{UTS}) for the UD-CFRP at -196 °C (3200 MPa) was approximately 40% higher than that at 20 °C (2300 MPa; i.e., $\Delta\sigma_{UTS} = 900$ MPa). This suggests that CFRPs are strengthened at lower temperatures and that low-temperature embrittlement does not occur. Similar results have been reported previously, although no clear explanation was provided [9]. It was reported that CFRPs with unidirectional $[90]_{10}$ laminate dramatically increased tensile stress (over 100%) at a low temperature of -60 °C [10].

The tensile properties of the epoxy at -196 °C were investigated to understand the high tensile strength of the UD-CFRP at low temperatures. Fig. 6 shows the ultimate tensile strengths of the epoxy at 20 and -196 °C. Like the tensile strength of the UD-CFRP, that of the epoxy increased by a factor of two at low temperatures compared with room temperature. Specifically, the tensile strength of the epoxy ($\Delta\sigma_{epoxy}$) after decreasing from 20 to -196 °C increased by approximately 350 MPa, which was approximately 38% of the $\Delta\sigma_{UTS}$ (900 MPa). The high tensile strength of the epoxy at -196 °C may be related to a reduction in the molecular mobility at low temperatures. In a related study [11], the fracture toughness of pure epoxy was found to increase with decreasing temperature,

(b) Tensile and fatigue test
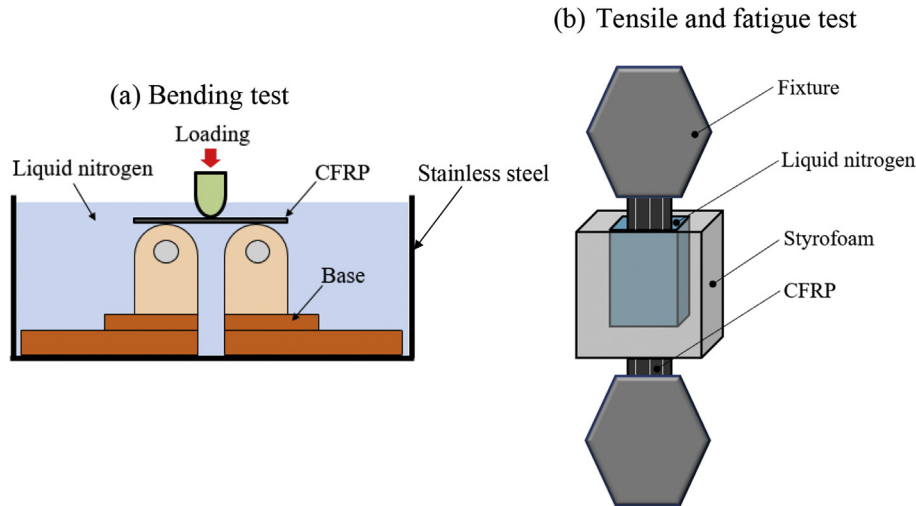
(a) Bending test

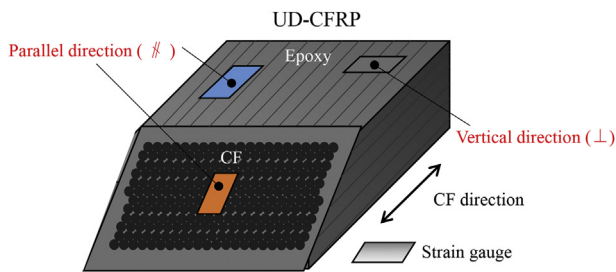Fig. 2. Schematic illustrations showing the testing setups for the bending, tensile, and fatigue tests.

Fig. 3. Schematic illustration showing the setup used to measure the strain of UD-CFRP at −196 °C.

with a 35% increase when the temperature decreased from 20 to −110 °C.

Although the high strength of the epoxy contributed to enhanced CRFP mechanical properties at low temperatures, the much lower value of $\Delta\sigma_{epoxy}$ compared with $\Delta\sigma_{UTS}$ indicates that other factors were also involved. It can be assumed that residual stresses lead to a high strength at low temperatures due to
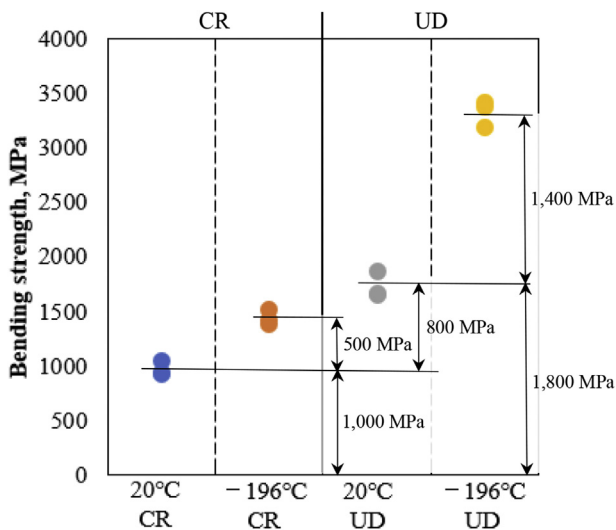

Fig. 4. Bending strengths for the CR-CFRP and UD-CFRP at 20 and −196 °C.

differences in the thermal expansion coefficients between the carbon fibers and epoxy, as discussed in a later section.

Fig. 7 shows the relationship between the stress amplitude and the number of cycles to failure (S_a vs. N_f) for the UD-CFRP at room temperature and −196 °C. The arrows on the S_a−N_f curves indicate that the specimen did not fail within 10^5 cycles (i.e., the endurance limit). The S_a−N_f curve for the UD-CFRP sample at −196 °C is higher than that at room temperature. However, the fatigue strength in the later fatigue stage, including the endurance limit, of the UD-CFRP at −196 °C is close to that for room temperature, as indicated by the dashed circle. In other words, the fatigue strength at −196 °C decreases during the later fatigue stage. This observation can be explained by assuming that the CFRP specimen is damaged at low temperatures, which is examined later in this section. On the other hand, the high fatigue strength of the sample at −196 °C in the early fatigue stage is related to the high tensile strength of the sample.

The S_a−N_f curves were further analyzed quantitatively using a power-law relationship between S_a and N_f:

$$S_a = \sigma_f N_f^{-b} \tag{2}$$

where σ_f is the fatigue strength coefficient and b is the fatigue exponent. In this case, a low b value and a high σ_f value result in high fatigue strength. The following expressions were determined for the UD-CFRP samples using a least-squares analysis: $S_a = 1792.4N_f^{-0.095}$ at −196 °C and $S_a = 1060.2N_f^{-0.053}$ at 20 °C. Thus, the σ_f and b values for the UD-CFRP at −196 °C were higher and lower than those at 20 °C, respectively. Overall, the analysis indicates that CFRPs have a high fatigue strength at −196 °C. To understand the failure characteristics of CFRPs at low temperatures, the fracture surface was observed using scanning electron microscopy (SEM) after fatigue testing (e.g., after approximately 10^2 and 10^4 cycles), as shown in Fig. 7.

Fig. 8 shows the SEM micrographs of the fractured surfaces for the UD-CFRP specimens after fracturing during the early (about 200 cycles) and later (about 15,000 cycles) fatigue stages. The observed fracture modes were obviously different for the two fracture stages. In the later fatigue stage, the epoxy strongly adhered to the carbon fibers, and fatigue failure occurred mainly in the epoxy as a result of material degradation. This type of fracturing may reduce the fatigue strength at later fatigue stages. In contrast, de-bonded and pulled-out fibers were observed at the early fatigue stage, which agrees with a previous report [12]. It is noted that in the present case, no
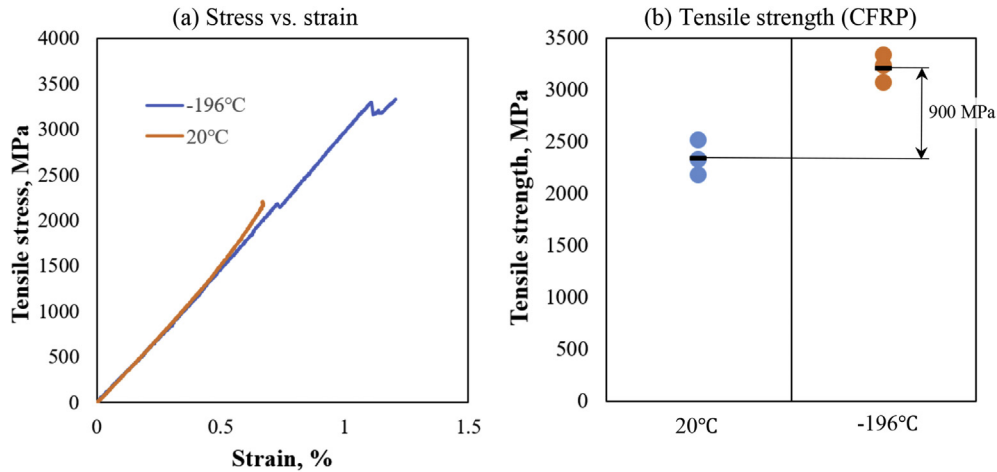
Fig. 5. (a) Representative stress–strain curves and (b) the ultimate tensile strengths of the UD-CFRP at 20 and −196 °C.
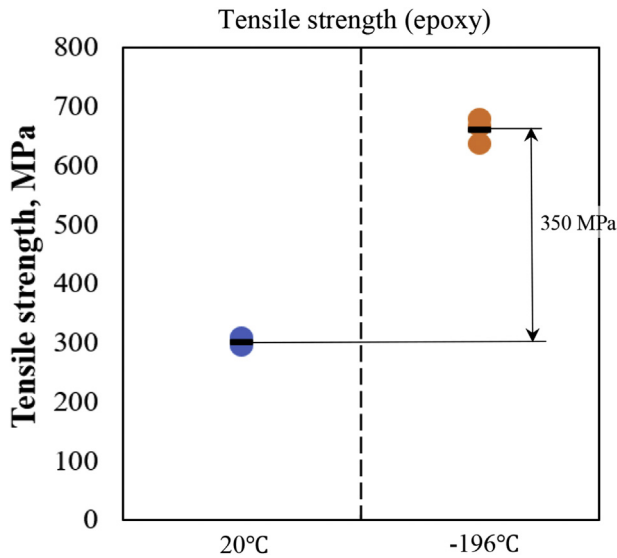

Fig. 6. Ultimate tensile strengths of the epoxy at 20 and −196 °C.

clear temperature effect is detected, while in a previous work, at a given impact energy, the delamination area increased as the temperature was lowered [13]. The CFRP rods are sometimes used to reinforce concrete beams, and the high cyclic fatigue properties of those beams were investigated at room temperature and −28 °C. The fatigue strength of concrete beams was enhanced, but the bond between the CFRP rods and concrete weakened at lower temperatures during cyclic loading [14]. Epoxy adhesives used to form the bonds between CFRPs and concrete are sensitive to temperature, such that the bond properties deteriorate rapidly at high temperatures, e.g., rapid loss of strength was reported as epoxy temperature increased beyond 60 °C [15].

3.2. Strain characteristics

To understand the material properties of the CFRP specimens in detail, the low-temperature strain characteristics of the UD-CFRP were examined. Fig. 9 shows the strain values for the CFRPs as measured using the strain gauges depicted in Fig. 3 (i.e., strain measured in the areas of the epoxy and carbon fibers). The strain measured perpendicular to the carbon fiber direction was higher

than that measured in the parallel direction. Furthermore, the strain in the epoxy area was higher than that in the carbon fiber region. These differences in strains resulted in the generation of internal stresses, which caused a change in the mechanical strength. The FE analyses were performed to further understand the strain characteristics of the UD-CFRP.

Fig. 10 depicts the von-Mises strain (ε_{von}) distribution in a cross-section of a UD-CFRP specimen. It is noted that the FE model was designed with a high magnification under the same carbon fiber volume fraction. The strain value was estimated from:

$$\varepsilon_{\text{von}} = \{1/(1+\nu)\} \times \left[0.5\left\{(\varepsilon_1 - \varepsilon_2)^2 + (\varepsilon_2 - \varepsilon_3)^2 + (\varepsilon_3 - \varepsilon_1)^2\right\}\right]^{0.5} \quad (3)$$

where ν is Poisson's ratio and ε_{x} is the principle strain. A high strain distribution can be seen in the epoxy around the carbon fibers. This can be explained from the different thermal expansion coefficients of the (high) epoxy and the (low) carbon fibers. In contrast, no clear strain was detected in the carbon fibers due to their high Young's modulus. The high strain in the epoxy generated a compressive
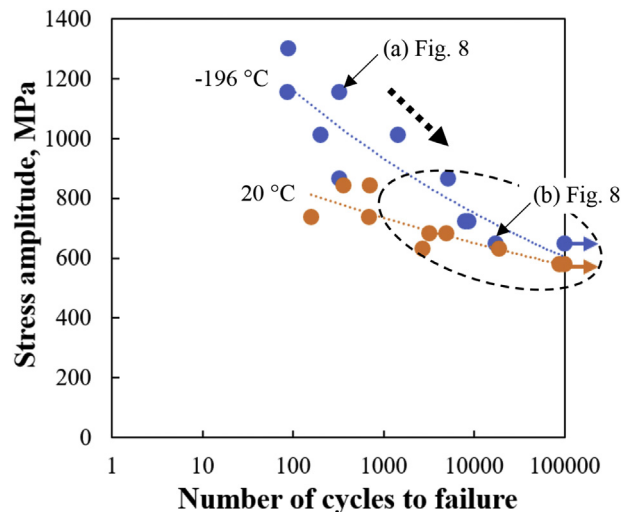

Fig. 7. Relationships between the stress amplitude and number of cycles to failure for the UD-CFRP at 20 and −196 °C.
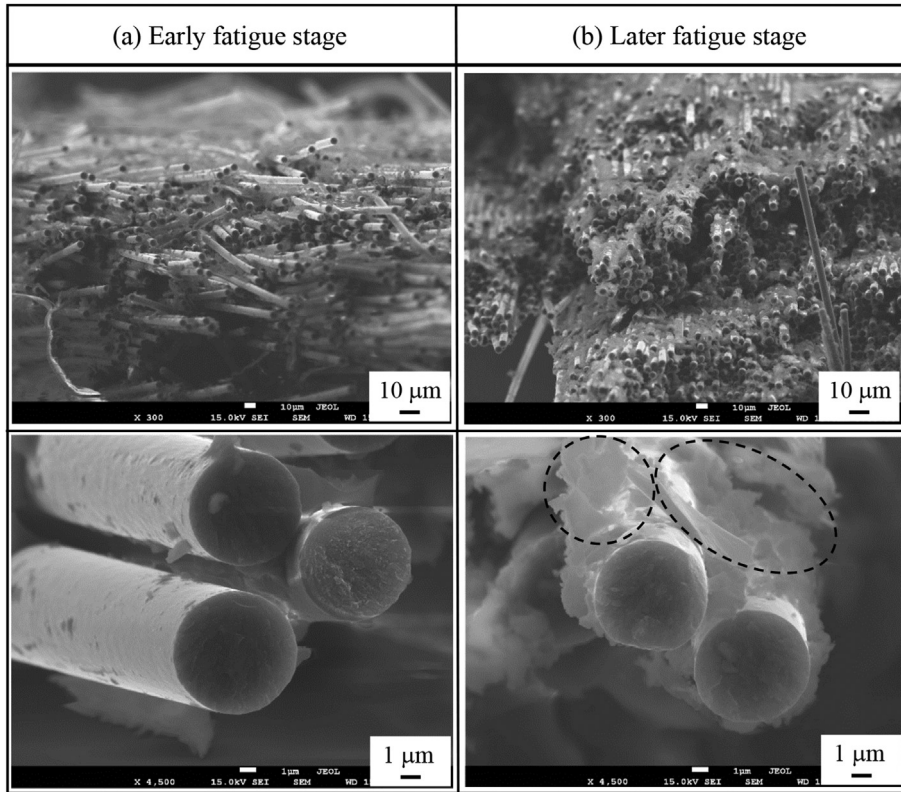
Fig. 8. SEM images of the fracture surfaces for the UD-CFRP after the tensile tests.
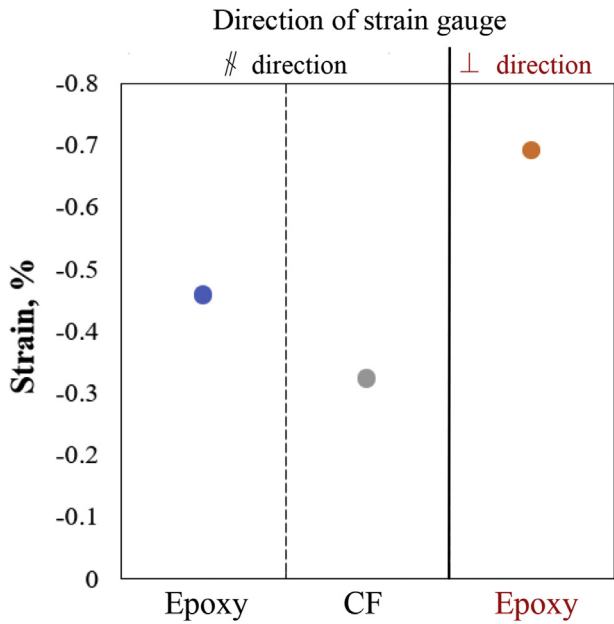

Fig. 9. Strain values of the epoxy and carbon fiber regions of the UD-CFRP at −196 °C measured as shown in Fig. 3.

stress, leading to the improved CFRP mechanical properties at low temperatures.

3.3. Numerical analysis

A previous study [16] assessed the tensile strength of carbon fibers using a multiple regression analysis by considering various
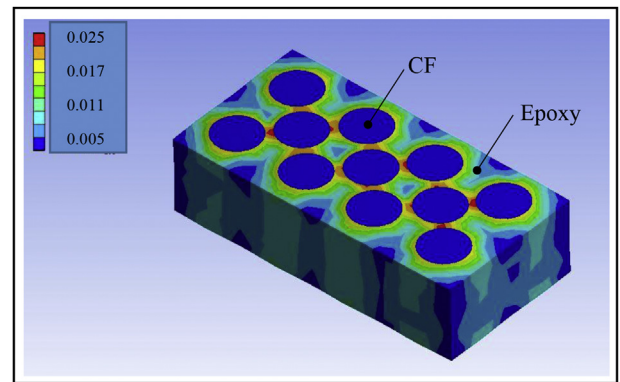

Fig. 10. von-Mises strain distribution of UD-CFRP at −196 °C determined from the FE analysis.

material parameters, including the fracture strain, elastic constant, wettability of carbon fiber on the resin, Vickers hardness, and carbon fiber type (UD or CR). To numerically estimate the tensile strength of the UD-CFRP (σ_{CFRP-n}) at low temperatures, a compound-law analysis was performed using the formula:

$$\sigma CFRP_{-n} = \sigma_f V_f + \sigma_m V_m, \tag{3a}$$

where σ_f and σ_m are the tensile strengths of the carbon fiber and epoxy, respectively, and V_f and V_m are their respective volume fractions. The material parameters used in the estimation were as follows: $\sigma_f = 3530$ MPa (carbon fiber) [17]; $\sigma_m = 300$ MPa (epoxy; Fig. 6); $V_f = 60\%$; and $V_m = 40\%$. Thus, the approximate value for the σ_{CFRP-n} was 2240 MPa, which agrees relatively well with the experimental results ($\sigma_{CFRP} = 2300$ MPa), see Table 1. However, the

Table 1
Results of the numerical analysis for the tensile strength of CFRP at 20 and −196 °C.

Tensile strength, MPa			
at −196 °C		at 20 °C	
Experimental σ_{CFRP}	Numerical σ_{CFRP-n}	Experimental σ_{CFRP}	Numerical σ_{CFRP-n}
2300	2240	3200	3123

estimated σ_{CFRP-n} was much lower than the tensile strength at −196 °C (3200 MPa), suggesting that conventional compound-law analyses may not be appropriate in this case. This low estimate could be related to the absence of thermal stresses (internal strain) in the model.

To address this issue, the compound law was modified based on several material properties at −196 °C (i.e., thermal stress and $\Delta\sigma_{epoxy}$ value). To obtain information about the CFRP thermal stress, it is necessary to determine the thermal expansion coefficient (α). Since no α values are available for the epoxy and carbon fiber, the α values were estimated using the formula:

$$\alpha = \varepsilon / \Delta T \tag{4}$$

with

$$\Delta T = T_1 - T_2 \tag{4a}$$

where ε is the strain and ΔT is the temperature range for the UD-CFRP. As shown in Fig. 9, the strain value of the UD-CFRP in the direction of the carbon fibers was approximated as a constant value of −0.4% [i.e., $\varepsilon = (\varepsilon_{epoxy} + \varepsilon_{CF})/2$]. Based on the obtained values of ε and ΔT, α was estimated as $-18.5 \times 10^{-6}/°C$. Furthermore, the thermal stresses of the carbon fiber (σ_{t-f}) and epoxy (σ_{t-m}) were calculated based on their Young's moduli and thermal strains ($\Delta T\alpha$):

$$\sigma_{t-f} = E_f \, \Delta T \left(\alpha - \alpha_f\right) \quad \text{for carbon fiber} \tag{5}$$

and

$$\sigma_{t-m} = E_m \, \Delta T \, (\alpha - \alpha_m) \quad \text{for epoxy} \tag{6}$$

Using Eqs. (5) and (6), the thermal stresses for the carbon fiber and epoxy were obtained as $\sigma_{t-f} = -899.2$ MPa and $\sigma_{t-m} = 16.3$ MPa, respectively. These estimates suggest that a high compressive stress and low tensile stress are created during the cooling process in the carbon fiber and epoxy, respectively. These stresses generate a residual stress (σ_r) at low temperatures of:

$$\sigma_r = \sigma_{t-f}V_f + \sigma_{t-m}V_m \tag{7}$$

The value of σ_r estimated from Eq. (7) was −533.0 MPa. The tensile strength for the UD-CFRP was significantly enhanced because of the high residual compressive stress.

Based upon the above results, the conventional compound law [Eq. (3)] was modified to consider the residual stress (σ_r) and tensile strength of the epoxy ($\Delta\sigma_{epoxy}$) as:

$$\sigma - 196^oC = \sigma CFRP_{-n} - \sigma_r + \Delta\sigma_{epoxy} \tag{8}$$

$$= V_f\left(\sigma_f + \sigma_{t-f}\right) + V_m(\sigma_m + \sigma_{t-m}) + \Delta\sigma_{epoxy} \tag{8a}$$

Using Eq. (8), the ultimate tensile strength for the UD-CFRP at −196 °C was approximated as 3123 MPa, which is in good agreement with the experimentally obtained tensile strength (3200 MPa). Thus, Eq. (8) may be applied to approximate the tensile strength of CFRPs at low temperatures. Overall, the results suggest that the residual compressive stress and tensile strength of the epoxy play important roles in determining the tensile properties of CFRPs at low temperatures. The obtained numerical analyses at room temperature and at −196 °C are summarized in Table 1.

4. Conclusion

The mechanical properties of CFRPs with a thermoset resin (epoxy) were examined experimentally and numerically to understand the material properties of CFRPs at low temperatures. Based on the obtained results, the following conclusions were drawn.

The mechanical properties of the UD-CFRP and CR-CFRP composites containing 60% carbon fiber were different. The bending strength of the UD-CFRP was approximately twice that of the CR-CFRP. The higher bending strength of the UD-CFRP is directly attributed to the greater proportion of carbon fiber oriented along the loading direction (60% for UD-CFRP vs. 30% for CR-CFRP). The low temperature (−196 °C) tensile and fatigue strengths of the UD-CFRP were more than 1.5 times greater than those at 20 °C. Similar to the UD-CFRP, the mechanical properties of the epoxy were enhanced after decreasing the temperature. The differences between the thermal expansion rates for carbon fiber and epoxy generated a residual compressive stress in the UD-CFRP at −196 °C. The conventional compound law was modified to estimate the ultimate tensile strength of CFRPs at −196 °C considering the residual compressive stress of the carbon fiber and the tensile strength of the epoxy at low temperatures. The modified compound law was found to well estimate the tensile strength for the UD-CFPR at low temperatures.

Declaration of Competing Interest

The authors declare no conflict of interest.

References

[1] J.L. Puente, R. Zaera, C. Navarro, The effect of low temperatures on the intermediate and high velocity impact response of CFRPs, Compos. B Eng. 33 (2002) 559–566.
[2] P.K. Dutta, Low temperature compressive strength of glass-fiber-reinforced polymer composites, J. Offshore Mech. Arct. Eng. 116 (1994) 167–172.
[3] Y. Miyano, M. Nakada, H. Kudoh, Prediction of tensile fatigue life for unidirectional CFRP, in: Progress in Durability Analysis of Composite Systems, Reifsnider & Cardon, 1998, pp. 303–308.
[4] R. Prakash, Significance of defects in the fatigue failure of carbon fibre reinforced plastics, Fibre Sci. Technol. 14 (1981) 171–181.
[5] M. Okayasu, T. Yamazaki, K. Ota, K. Ogi, T. Shiraishi, Mechanical properties and failure characteristics of a recycled CFRP under tensile and cyclic loading, Int. J. Fatigue 55 (2013) 257–267.

[6] Y. Huawen, C. Konig, T. Ummenhofer, Q. Shizhong, R. Plum, Fatigue performance of tension steel plates strengthened with prestressed CFRP laminates, J. Compos. Constr. 14 (2010) 609–615.

[7] M.D. Ludovico, F. Piscitelli, A. Prota, M. Lavorgna, G. Mensitieri, G. Manfredi, Improved mechanical properties of CFRP laminates at elevated temperatures and freeze–thaw cycling, Constr. Build. Mater. 31 (2012) 273–283.

[8] S.S. Tompkins, Thermal expansion of selected graphite-reinforced polyimide-, epoxy-, and glass-matrix composites, Int. J. Thermophyics 8 (1987) 119–132; a K. Murayama, T. Tanaka, Thermal expansion of carbon fiber reinforced composites, Zairyo 25 (1976) 17–21.

[9] M.A. Torabizadeh, Tensile, compressive and shear properties of unidirectional glass/epoxy composites subjected to mechanical loading and low temperature services, Indian J. Eng. Mater. Sci. 20 (2013) 299–309.

[10] T. Gómez-del Río, E. Barbero, R. Zaera, C. Navarro, Dynamic tensile behaviour at low temperature of CFRP using a split Hopkinson pressure bar, Compos. Sci. Technol. 65 (2005) 61–71.

[11] S.C. Kunz, P.W.R. Beaumont, Low-temperature behaviour of epoxy-rubber particulate composites, J. Mater. Sci. 16 (1981) 3141–3152.

[12] H.J. Kwon, P.-Y.B. Jar, Z.J. Xia, Residual toughness of poly (acrylonitrile-butadience-styrene) (ABS) after fatigue loading-effect of uniaxial fatigue loading, Mater. Sci. 39 (2004) 4821–4828.

[13] T. Gómez-del Río, R. Zaera, E. Barbero, C. Navarro, Damage in CFRPs due to low velocity impact at low temperature, Compos. B Eng. 36 (2005) 41–50.

[14] R. Saiedi, A. Fam, M.F. Green, Behavior of CFRP-prestressed concrete beams under high-cycle fatigue at low temperature, J. Compos. Constr. 15 (2011) 482–489.

[15] J.C.P.H. Gamage, M.B. Wong, R. Al-Mahaidi, Performance of CFRP strengthened concrete members under elevated temperatures, in: Proc. Int. Symp. Bond Behaviour FRP in Struct. (BBFS 2005), 2005, pp. 113–118.

[16] M. Okayasu, Y. Tsuchiya, H. Arai, Experimentally and analyzed property of carbon fiber reinforced thermoplastic and thermoset plates, J. Mater. Sci. Res. 7 (2018) 12–21.

[17] T. Tagawa, T. Miyata, Size effect on tensile strength of carbon fibers, Mater. Sci. Eng. A 238 (1997) 336–342.